Available online at www.sciencedirect.com
SCIENCE DIRECT®
PERGAMON
Polyhedron 22 (2003) 1759–1763
POLYHEDRON
www.elsevier.com/locate/poly

Reaction of $[Mn_{12}O_{12}(O_2CR)_{16}(H_2O)_4]$ single-molecule magnets with non-carboxylate ligands

Nicole E. Chakov [a], Khalil A. Abboud [a], Lev N. Zakharov [b], Arnold L. Rheingold [b], David N. Hendrickson [c], George Christou [a,*]

[a] Department of Chemistry, University of Florida, P.O. Box 117200, Gainesville, FL 32611-7200, USA
[b] Department of Chemistry, University of Delaware, Newark, DE 19716, USA
[c] Department of Chemistry and Biochemistry, University of California at San Diego, La Jolla, San Diego, CA 92083-0358, USA

Received 6 October 2002; accepted 2 January 2003

Abstract

New derivatives of the $[Mn_{12}O_{12}(O_2CR)_{16}(H_2O)_4]$ family of single-molecule magnets (SMMs) have been obtained through the use of the non-carboxylate ligand benzenesulfonate. The reaction of $[Mn_{12}O_{12}(O_2CMe)_{16}(H_2O)_4]$ with eight equivalents of benzenesulfonic acid gives $[Mn_{12}O_{12}(O_2CMe)_8(O_3SPh)_8(H_2O)_4]$. The cluster possesses an $S = 10$ ground state and exhibits out-of-phase ac susceptibility signals characteristic of a SMM. The reaction of $[Mn_{12}O_{12}(O_2CMe)_8(O_3SPh)_8(H_2O)_4]$ with diphenylphosphinic acid gives $[Mn_4O_4(O_2PPh_2)_6]$, containing a manganese-oxo cubane core structure.

Keywords: Single-molecule magnet; Mn cluster; Benzenesulfonic acid

1. Introduction

Following the discovery that single-molecules of $[Mn_{12}O_{12}(O_2CMe)_{16}(H_2O)_4]$ display superparamagnetic properties and thus function as magnets below their blocking temperatures, considerable attention has been devoted towards both the understanding of this novel magnetic phenomenon of single-molecule magnetism and the pursuit of other complexes that exhibit similar properties [1–4]. Rather than arising from intermolecular interactions and long-range ordering, the properties of a single-molecule magnet (SMM) originate from both a high-spin ground state (S) and a large, negative (easy axis type) magnetoanisotropy, resulting in a significant energy barrier to relaxation (reorientation) of the magnetization vector, as required for a SMM.

Recently attempts have been made to derivatize the Mn_{12} complexes with non-carboxylate ligands in a site-specific manner, enhancing reactivity at selected sites and making regioselective reactions possible. Progress along these lines includes the site-specific replacement of some of the carboxylate groups on $[Mn_{12}O_{12}(O_2CR)_{16}(H_2O)_4]$ with nitrate [5] or diphenylphosphinate [6] anions to give $[Mn_{12}O_{12}(NO_3)_4(O_2CR)_{12}(H_2O)_4]$ ($R = CH_2Bu^t$ and Ph) and $[Mn_{12}O_{12}(O_2CMe)_8(O_2PPh_2)_8(H_2O)_4]$, respectively. Since then, the related complex $[Mn_{12}O_{12}(O_2CPh)_{12}(O_2P(OPh)_2)_4(H_2O)_4]$ has been reported by others [7]. These studies represent limited success, because substitution of just all axial or all equatorial carboxylate ligands with non-carboxylate groups has not been achieved. This has now been accomplished, however, by the introduction of benzenesulfonate groups, $PhSO_3^-$, into all of the axial sites of the Mn_{12} cluster. The complex, $[Mn_{12}O_{12}(O_2CMe)_8(O_3SPh)_8(H_2O)_4]$, functions as a SMM, having a high-spin ground state, $S = 10$, and a large, negative magnetic anisotropy, D.

Reactivity studies on this new Mn_{12} complex have led to the preparation of a tetranuclear Mn cluster, $[Mn_4O_4(O_2PPh_2)_6]$, possessing a manganese-oxo cubane core $[Mn_4O_4]^{6+}$. The cluster contains non-carboxylate diphenylphosphinate ligands and maintains the central cubane core of the Mn_{12} cluster, but it is not a SMM.

* Corresponding author. Tel.: +1-352-392-8314; fax: +1-352-392-8757.
E-mail address: christou@chem.ufl.edu (G. Christou).

0277-5387/03/$ - see front matter
doi:10.1016/S0277-5387(03)00222-5

2. Experimental

2.1. Syntheses

All manipulations were performed under aerobic conditions using materials as received. $[Mn_{12}O_{12}(O_2CMe)_{16}(H_2O)_4]$ (**1**) was prepared as previously described [8].

2.1.1. Preparation of $[Mn_{12}O_{12}(O_2CMe)_8(O_3SPh)_8(H_2O)_4]\cdot 4CH_2Cl_{12}$ (**2**)

Complex **2** was obtained by ligand substitution of **1** with eight equivalents of benzenesulfonic acid ($PhSO_3H$) in MeCN. Acetic acid was removed from the system by multiple additions and removals of toluene under vacuum, leading to the isolation of **2** in 96% yield. The final residue was recrystallized from CH_2Cl_2/hexanes.

2.1.2. Preparation of $[Mn_4O_4(O_2PPh_2)_6]$ (**3**)

The reaction of **2** with eight equivalents of diphenylphosphinic acid (Ph_2PO_2H) in MeCN leads to the isolation of **3**. Multiple additions and removals of toluene under vacuum drive the reaction by removal of acetic acid. The final residue is crystallized from CH_2Cl_2/toluene, with precipitation of the excess ligands, diphenylphosphinic acid and benzenesulfonic acid.

3. Results and discussion

3.1. Description of structures

3.1.1. $[Mn_{12}O_{12}(O_2CMe)_8(O_3SPh)_8(H_2O)_4]\cdot 4CH_2Cl_2$ (**2**)

Complex **2** crystallizes in the triclinic space group $P\bar{1}$ and possesses an overall geometry similar to that of **1**, with a central $[Mn^{IV}_4O_4]$ cubane held within a non-planar ring of eight Mn^{III} ions by eight μ_3-O^{2-} ions (Fig. 1). The eight equatorial sites of the complex are occupied by $MeCO_2^-$ groups while the $PhSO_3^-$ ligands are located at the axial sites above and below the disk-like core structure [9]. There is near parallel alignment of each of the Jahn-Teller (JT) elongated axes of the eight Mn^{III} ions perpendicular to the plane of the disk, accounting for a significant magnetic anisotropy in the z direction. The occupation of the axial positions by the $PhSO_3^-$ ligands rather than the $MeCO_2^-$ groups is rationalized on the basis of relative basicities. The pK_a value of $PhSO_3H$ is 2.55 while that of $MeCO_2H$ is 4.76. The more basic, stronger donor $MeCO_2^-$ ligands favor occupation of the equatorial sites where shorter, stronger Mn–O bonds can be formed [9]. The $PhSO_3^-$ ligands bridge either $Mn^{III}Mn^{III}$ or $Mn^{III}Mn^{IV}$ pairs and thus have one or both of their O atoms on the JT elongation axes.

Comparison of **2** with the related clusters $[Mn_{12}O_{12}(O_2CMe)_{16}(H_2O)_4]$ (**1**) and $[Mn_{12}O_{12}(O_2CMe)_8(O_2PPh_2)_8(H_2O)_4]$ (**4**) reveals that there is no significant distortion of the $[Mn_{12}O_{12}]^{16+}$ core upon coordination of the non-carboxylate benzenesulfonate groups (Table 1). The apparent lack of distortion is in contrast to that seen within the core of **4** in which the $Mn^{III}\cdots O^{2-}\cdots Mn^{III}$ bond angles differ significantly and the $Mn^{III}\cdots Mn^{III}$ bond distances are on average 0.1 Å longer than the corresponding values of **1**. Additional differences are reflected in the linearity of the Mn_4 units that span the core of the cluster, with **1** and **2** having angles of the type $Mn^{III}\cdots Mn^{IV}\cdots Mn^{IV}$ equal to almost 180° while the corresponding angle in **4** is only ~171° [7]. The similarity of complexes **1** and **2**, and the difference between them and **4** are likely reflective of the distribution of ligands around the cluster. In **4**, the acetate groups at the four axial $Mn^{III}Mn^{III}$ and four of the equatorial $Mn^{III}Mn^{III}$ carboxylate sites have been replaced by relatively bulky diphenylphosphinate groups, giving rise to a distortion of the core of the complex from steric effects.

3.1.2. $[Mn_4O_4(O_2PPh_2)_6]$ (**3**)

Complex **3** crystallizes in the cubic space group $P2_13$ with four crystallographically independent molecules in the unit cell, each slightly different with respect to the orientation of the phenyl groups of the diphenylphosphinate ligands [10]. The cluster consists of a cubane $[Mn_4O_4]^{6+}$ core in which there is one unique and three symmetry-related Mn ions (Fig. 2). Diphenylphosphinate ligands that bridge Mn pairs across each of the six Mn_2O_2 faces complete the coordination sphere of the complex. In contrast to the related distorted-cubane clusters with $[Mn_4O_3X]$ cores, in which there are clear JT elongation axes at the Mn^{III} ions, there are no distinct JT elongated bonds in the case of **3** [11]. A bond valence sum analysis indicates that the four Mn oxidation states are the same, which could be due to an electronically delocalized system or a static disorder of trapped-valence Mn^{III} and Mn^{IV} sites.

Comparison of the Mn···Mn separations across the faces of the cube with related Mn complexes having cubane cores indicates that the distances in **3** most closely resemble those in the central $[Mn_4O_4]^{16+}$ core of members of the Mn_{12} family. Averaged over the four independent molecules of the unit cell, the mean Mn···Mn distance is 2.93 Å. Similar distances are found in Mn_{12} complexes while those in the distorted-cubane Mn_4 complexes are slightly shorter. Unlike **3,** the Mn_{12} complexes have no carboxylate-bridged Mn_2 pairs in the cubane core. Comparison of the O···O distances of the carboxylate and non-carboxylate ligands in **3** shows that diphenylphosphinate groups may be preferred for formation of the cubane complex. The average O···O distances for the bridging ligands acetate, benzenesulfo-

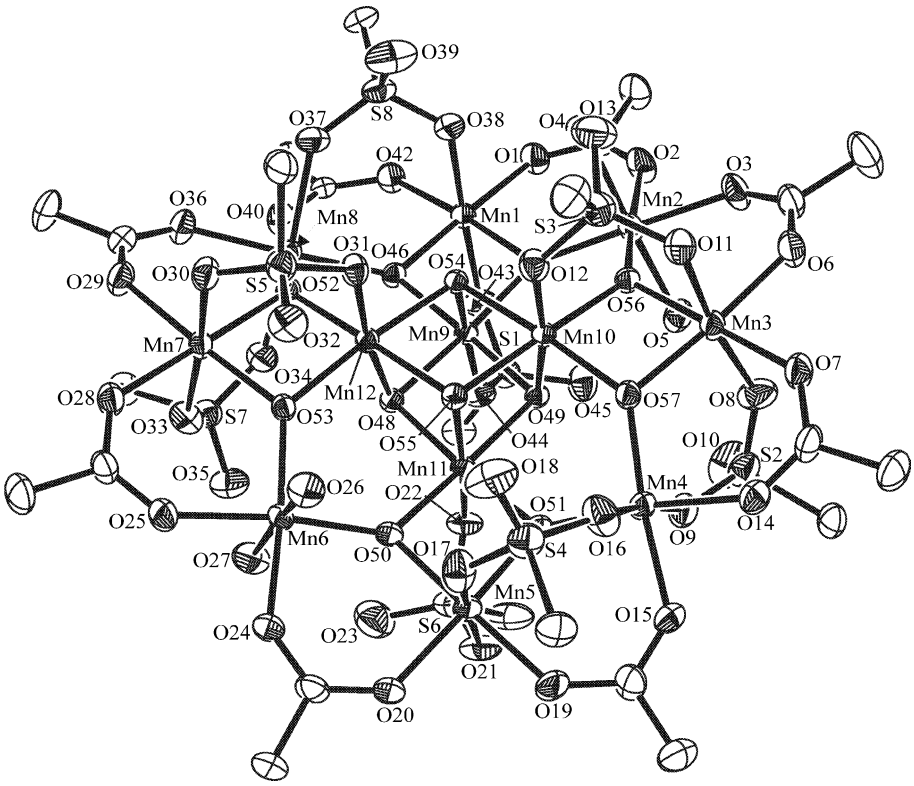

Fig. 1. Labeled ORTEP representation of complex **2** at the 50% probability level. For clarity, only the *ipso* carbon atom of each phenyl ring is included.

nate, and diphenylphosphinate are 2.24, 2.42 and 2.57 Å, respectively.

3.2. Magnetism studies

3.2.1. $[Mn_{12}O_{12}(O_2CMe)_8(O_3SPh)_8(H_2O)_4]\cdot 4CH_2Cl_2$ (**2**)

Variable-temperature dc magnetic susceptibility (χ_M) data were collected on **2** in the 2.00–300 K range in a 5 KG (0.5 T) magnetic field. The $\chi_M T$ versus T behavior is similar to those of previously studied $[Mn_{12}O_{12}(O_2CR)_{16}(H_2O)_4]$ complexes with $S = 10$ ground states, exhibiting a nearly temperature-independent value of 20–21 $cm^3\ K\ mol^{-1}$ in the 150–300 K range which then increases rapidly to a maximum value of 44–45 $cm^3\ K\ mol^{-1}$ at ~ 20 K before decreasing rapidly at lower temperatures. The maximum indicates a large ground state spin (S) value, and the low temperature decrease is primarily due to Zeeman and zero-field splitting effects.

To probe the magnetic properties of **2**, ac magnetic susceptibility measurements in the 1.8–10 K range were made in a 3.5 G ac field oscillating at frequencies up to 1000 Hz (Fig. 3). Both the frequency-dependent decrease at $T < 10$ K in the in-phase ($\chi'_M T$) signal as well as the concomitant appearance of a frequency-dependent out-of-phase (χ''_M) signal indicate that the magnetic

Table 1
Selected bond lengths (Å) and angles (°) for complexes **1**, **2**, and **4**

Parameter	**1**	**2**	**4**
$Mn^{III}\cdots Mn^{III}$	3.32, 3.42	3.35–3.45, 3.37–3.45	3.41, 3.55
$Mn^{IV}\cdots Mn^{IV}$	2.82, 2.93	2.80–2.81, 2.94–2.95	2.85, 2.95
$Mn^{IV}\cdots O^{2-}$ (Inner core)	1.90, 1.91, 1.92	1.86–1.88, 1.92–1.94, 1.92–1.93	1.89, 1.90, 1.96
$Mn^{IV}\cdots O^{2-}$ (Outer core)	1.86, 1.88	1.85–1.87, 1.86–1.87	1.86, 1.86
$Mn^{III}\cdots O^{2-}$ (Outer core)	1.88, 1.89, 1.90, 1.90	1.88–1.90, 1.90–1.91, 1.89–1.91, 1.88–1.91	1.87, 1.89, 1.93, 1.99
$Mn^{III}\cdots Mn^{IV}$	2.76, 3.44, 3.45	2.79–2.80, 3.42–3.45, 3.42–3.47	2.77, 3.42, 3.45
$Mn^{III}\cdots O^{2-}\cdots Mn^{III}$	122.8, 129.6	123.3–130.1, 126.5–130.1	129.4, 130
$Mn^{III}\cdots O^{2-}\cdots Mn^{IV}$	94.1–95.5, 132.6–133	95.4–97.0, 130.6–132.7	93.9–95.5, 127.2–133.1
$Mn^{IV}\cdots O^{2-}\cdots Mn^{IV}$	95.1–95.4, 99.7	95.1–95.9, 99.3–99.9	95.3–97.2, 99.3
$Mn^{III}\cdots Mn^{IV}\cdots Mn^{IV}$	178.4	176–178.2	171.4
$Mn^{III}\cdots Mn^{III}\cdots Mn^{III}$	122.9, 138.0	118.8–122.2, 139.2–140.9	116.3, 138.4

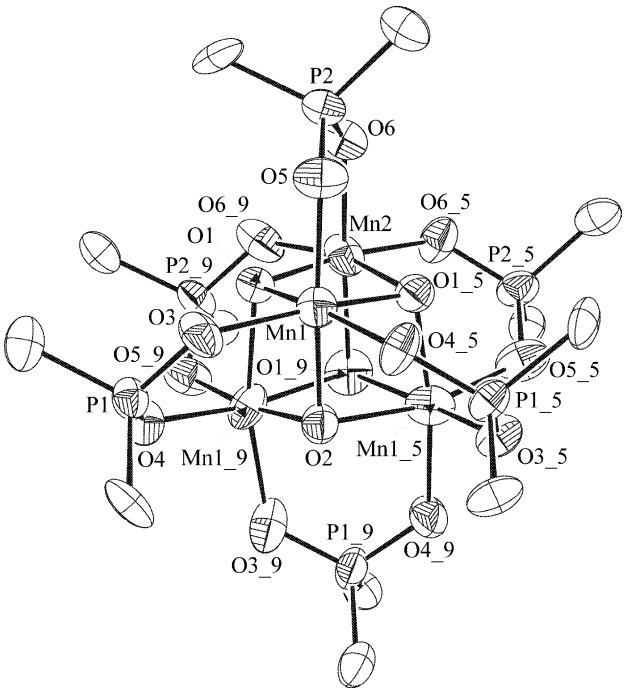

Fig. 2. Labeled ORTEP representation of one of the four molecules in the unit cell of complex **3** at the 50% probability level. For clarity, only the *ipso* carbon atom of each phenyl ring is included.

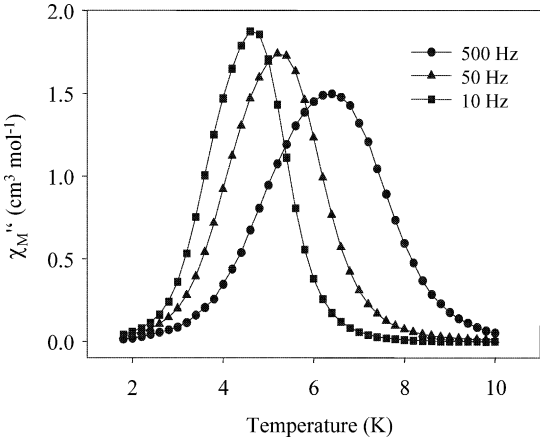

Fig. 3. Out-of-phase (χ_M'') ac susceptibility versus temperature plot for **2** at the indicated frequencies.

relaxation rate becomes comparable with the rate of the oscillating field. The plateau value of the in-phase ac signal above ~ 8 K is consistent with an $S = 10$ ground state with g ~ 2. Frequency-dependent χ_M'' signals have been observed in the ac susceptibility studies of all Mn_{12} SMMs and are considered a diagnostic signature of the single-molecule magnetism property. Hence, complex **2** retains the SMM properties of a typical Mn_{12} cluster. There is only one χ_M'' peak at each ac frequency, consistent with the absence of JT isomerism. The latter is the phenomenon whereby some Mn_{12} molecules possess an abnormally oriented JT axis that is equatorial rather than axial with respect to the Mn_{12} disk, causing an increase in the magnetization relaxation rate and a χ_M'' peak at correspondingly lower temperatures [12,13]. This thus leads to the so-called faster-relaxing Mn_{12} species.

At the temperature of the χ_M'' peak maximum, the magnetization relaxation rate ($1/\tau$) equals the angular frequency ($2\pi\nu$) of the ac field. Thus, the χ_M'' versus T plots at different frequencies (ν) provide $1/\tau$ versus T data, and a kinetic analysis can be performed using the Arrhenius relationship (Eq. (1)) [14].

$$\ln\frac{1}{\tau} = -\frac{U_{\text{eff}}}{kT} + \ln\frac{1}{\tau_o} \tag{1}$$

Parameters determined from a fit of the χ_M'' data to the Arrhenius equation include the effective energy barrier to magnetization relaxation (U_{eff}) and the pre-exponential term ($1/\tau_o$). Analysis indicates that U_{eff} for **2** is 45.6 cm^{-1} (65.5 K), a value within the normal range of 42–50 cm^{-1} (60–72 K) for the $[Mn_{12}O_{12}(O_2CR)_{16}(H_2O)_x]$ family.

3.2.2. *[$Mn_4O_4(O_2PPh_2)_6$] (3)*

DC magnetic susceptibility data were collected in the 5.00–300 K range on a powdered microcrystalline sample of **3** restrained in eicosane to prevent torquing. The $\chi_M T$ per molecule smoothly decreases from 6.58 cm^3 K mol^{-1} at 300 K to 0.78 cm^3 K mol^{-1} at 5 K. The value at 300 K is less than 9.75 cm^3 K mol^{-1}, the spin-only value expected for a $2Mn^{III}$, $2Mn^{IV}$ complex with non-interacting metal centers, indicating the presence of appreciable antiferromagnetic interactions between the manganese ions. Additional ac studies indicate no peak in the out-of-phase ac susceptibility. Hence, **3** does not function as a SMM. Like the dc measurements, in-phase ac studies suggest an $S = 0$ (or 1) ground state for complex **3**. Clear identification of the ground state is likely precluded by population of low-lying excited states. Further studies are required to further understand the magnetic properties of the complex.

4. Conclusions

In conclusion, site-selective substitution of all axial ligands from $[Mn_{12}O_{12}(O_2CR)_{16}(H_2O)_x]$ complexes has been achieved, with replacement of the carboxylate groups of **1** with $PhSO_3^-$ ligands. Incorporation of the non-carboxylate, S-based ligands is driven by the greater acidity of $PhSO_3H$ over $MeCO_2H$, with the less basic $PhSO_3^-$ ligands occupying axial sites with at least one O atom lying along a Mn^{III} JT elongation axis. Single-molecule magnetism properties of the benzenesulfonate-substituted complex are retained, with the complex possessing an $S = 10$ ground state and displaying frequency-dependent peaks in the out-of-phase magnetic

susceptibility. Complex **2** is also a potential starting point for further chemistry and may prove useful to access new SMMs as regioselective chemistry is likely to prove feasible with a variety of reagents. Such reactivity studies on **2** with diphenylphosphinic acid have afforded a clean route for the preparation of a tetranuclear cluster possessing a $[Mn_4O_4]^{6+}$ cubane core. Although **3** does not retain the SMM properties of its parent compound, it provides further insight into the behavior of **2** when treated with additional non-carboxylate ligands.

5. Supplementary material

Crystallographic data for the structural analysis have been deposited with the Cambridge Crystallographic Data Centre, CCDC No. 194416. Copies of this information may be obtained free of charge from The Director, CCDC, 12 Union Road, Cambridge, CB2 1EZ, UK (fax: +44-1223-336033; email: deposit@ccdc.cam.ac.uk or http://www.ccdc.cam.ac.uk).

Acknowledgements

This work was supported by NSF grant to G.C. and D.N.H.

References

[1] G. Christou, D. Gatteschi, D.N. Hendrickson, R. Sessoli, MRS Bull. 25 (2000) 66.
[2] R. Sessoli, H.-L. Tsai, A.R. Schake, S. Wang, J.B. Vincent, K. Folting, D. Gatteschi, G. Christou, D.N. Hendrickson, J. Am. Chem. Soc. 115 (1993) 1804.
[3] R. Sessoli, D. Gatteschi, A. Caneschi, M.A. Novak, Nature 365 (1993) 141.
[4] H.J. Eppley, H.-L. Tsai, N. de Vries, K. Folting, G. Christou, D.N. Hendrickson, J. Am. Chem. Soc. 117 (1995) 301.
[5] P. Artus, C. Boskovic, J. Yoo, W.E. Streib, L.-C. Brune, D.N. Hendrickson, G. Christou, Inorg. Chem. 40 (2001) 4199.
[6] C. Boskovic, M. Pink, J.C. Huffman, D.N. Hendrickson, G. Christou, J. Am. Chem. Soc. 123 (2001) 9914.
[7] T. Kuroda-Sowa, S. Fukuda, S. Miyoshi, M. Maekawa, M. Munakata, H. Miyasaka, M. Yamashita, Chem. Lett. (2002) 682.
[8] T. Lis, Acta Crystallogr. B 36 (1980) 2042.
[9] M. Soler, P. Artus, K. Folting, J.C. Huffman, D.N. Hendrickson, G. Christou, Inorg. Chem. 40 (2001) 4902.
[10] W.F. Ruettinger, C. Campana, G.C. Dismukes, J. Am. Chem. Soc. 119 (1997) 6670.
[11] S. Wang, H.-L. Tsai, K.S. Hagen, D.N. Hendrickson, G. Christou, J. Am. Chem. Soc. 116 (1994) 8376.
[12] Z. Sun, D. Ruiz, N.R. Dilley, M. Soler, J. Ribas, K. Folting, M.B. Maple, G. Christou, D.N. Hendrickson, Chem. Commun. 19 (1999) 1973.
[13] S.M.J. Aubin, Z. Sun, H.J. Eppley, E.M. Rumberger, I.A. Guzei, K. Folting, P.K. Gantzel, A.L. Rheingold, G. Christou, D.N. Hendrickson, Polyhedron 20 (2001) 1139.
[14] M.A. Novak, R. Sessoli, in: L. Gunther, B. Barbara (Eds.), Quantum Tunneling of Magnetization—QTM'94, Kluwer Academic Publishers, Dordrecht, 1995, pp. 171–188.